

Charge Inversion and Flow Reversal in a Nanochannel Electro-osmotic Flow

R. Qiao and N. R. Aluru*

Department of Mechanical and Industrial Engineering, Beckman Institute for Advanced Science and Technology, University of Illinois at Urbana-Champaign, Urbana, Illinois 61801, USA

(Received 6 August 2003; published 10 May 2004)

Ion distribution and velocity profiles for electro-osmotic flow in a 3.49 nm wide slit channel with a surface charge density of -0.285 C/m^2 are studied using molecular dynamics simulations. Simulation results indicate that the concentration of the co-ion exceeds that of the counterion in the region 0.53 nm away from the channel wall, and the electro-osmotic flow is in the opposite direction to that predicted by the classical continuum theory. The charge inversion is mainly caused by the molecular nature of water and ions. The flow reversal is caused by the immobilization of counterions adsorbed on the channel wall and due to the charge inversion phenomena.

DOI: 10.1103/PhysRevLett.92.198301

PACS numbers: 82.39.Wj, 47.11.+j, 47.15.Gf, 82.45.-h

When an ionic solution is in contact with a charged surface, an electrical double layer (EDL) with a net positive or negative charge develops near the surface. If an external electrical field is applied in the direction tangential to the surface, the fluid will be dragged by the moving ions in the EDL and an electro-osmotic transport is generated. Because of its scalability and ease of control, electro-osmotic transport is a popular fluidic transport mechanism in micro and nanofluidic systems [1,2]. Various models have been proposed to predict the ion distribution and fluid flow in electro-osmotic transport [3]. However, many important physical effects (e.g., the discrete water molecule effect) are neglected in these models. As a result, the classical models fail to predict many experimental [4] and atomistic simulation results [5–7].

In this Letter, through detailed molecular dynamics simulations, we report on charge inversion and flow reversal of electro-osmotic transport in a slit silicon nanochannel. The charge inversion refers to the phenomena where the co-ion charge density exceeds the counterion charge density in a certain region of the EDL. The flow reversal refers to the phenomena where the electro-osmotic flow is in the opposite direction to the one typically expected. For example, when the surface is negatively charged and the external electrical field is in the positive direction, one typically expects the electro-osmotic flow to be in the positive direction. However, an electro-osmotic flow in the negative direction will be observed when the flow reversal occurs. Although the charge inversion phenomena have been explained by considering the finite size of the ion [8], the importance of the discreteness of the water molecules was seldom reported. Here, we present quantitative analysis showing how the nonelectrostatic ion-water interactions can contribute significantly to the charge inversion phenomena. The flow reversal is typically understood as a result of “superequivalent specific adsorption” of counterions [9]; i.e., the total charge of the counterions adsorbed on the charged surface by nonelectrostatic means exceeds the

surface charge. We show, however, that the flow reversal can occur even if the adsorption of counterions does not exceed the surface charge.

Figure 1 shows the schematic diagram of the system under investigation. The system consists of a slab of NaCl solution sandwiched between two channel walls (lateral dimensions: $4.66 \text{ nm} \times 4.22 \text{ nm}$). Each wall is made up of four layers of silicon atoms oriented in the 111 direction. The channel width, defined as the distance between the two innermost wall layers, is 3.49 nm. A total charge of $-70e$ is evenly distributed among the atoms of the innermost wall layers, giving an average surface charge density (σ_s) of -0.285 C/m^2 . Such a charge density can be considered high, but it is not impractical as the typical charge density of a fully ionized surface can exceed 0.3 C/m^2 in magnitude [10,11]. The system contains 108 Na^+ ions, 38 Cl^- ions, and 2144 water molecules. The extended simple point charge (SPC/E) model is used for water and the ions are modeled as charged Lennard-Jones (LJ) atoms. The LJ parameters for ion-ion and ion-water pairs were taken from [12], and those for the ion-Si and oxygen-Si pairs were obtained by using the linear combination rule and the Si-Si parameters from [13].

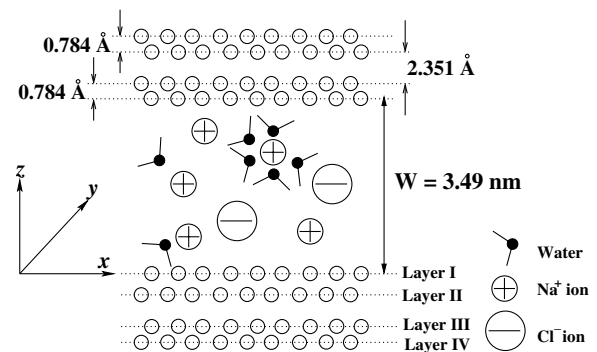


FIG. 1. A schematic of the channel system under investigation. For the coordinate system chosen, $z = 0$ corresponds to the layer I of the lower channel wall.

Simulations were performed with a modified Gromacs 3.0.5 [13]. Periodic boundary conditions are used in the x and y directions. A Nose thermostat [14] was used to maintain the fluid temperature at 300 K. To avoid biasing the velocity profile, only the velocity component in the direction orthogonal to the flow was thermostated [15]. The electrostatic interactions were computed by using the PME slab method [16]. Other simulation details can be found in [6]. Starting from a random configuration, the system was simulated for 2.0 ns to reach steady state, followed by a 15 ns production run. The flow was driven by an electric field, E_{ext} , applied in the x direction. Because of the extremely high thermal noise, a strong electric field ($E_{\text{ext}} = 0.55$ V/nm) was used so that the fluid velocity can be retrieved with reasonable accuracy [17]. The velocity and concentration profiles are obtained using the binning method.

Because of the symmetry of our system, the ion distribution is analyzed only in the lower portion of the channel by computing the mean force acting on the ions [18]. Only the z -direction mean force is computed as we are primarily interested in analyzing the average ion concentration across the channel. The mean force $f_i(z)$ acting on an ion i , located at a position z , is computed as the total force on ion i from all other particles in the system averaged over all configurations. $f_i(z)$ is denoted negative if it drives the ion towards the lower channel wall and positive, otherwise. The potential of mean force (PMF), denoted $w_i(z)$, for an ion i at a position z is computed by $w_i(z) = \int_z^{z_f} f_i(z') dz'$, where z_f is the reference plane (taken as the channel center plane here) at which the PMF is taken as zero. Within the limit of the classical statistical mechanics [19], the concentration of an ion i at a position z , denoted by $c_i(z)$, is related to the PMF by the Boltzmann distribution, $c_i(z) = c_i^{z_f} \exp[-w_i(z)/k_B T]$, where $c_i^{z_f}$, k_B , and T are the concentration of ion i at the reference plane, the Boltzmann constant and the temperature, respectively. To facilitate discussion, we decompose the total mean force into an electrostatic mean force and a nonelectrostatic mean force. In certain cases, we further decompose the nonelectrostatic mean force into several components arising from the interactions of the molecule (e.g., wall atoms, ion, or water) with the ion.

To measure the screening of the surface charge by the ions, we define a screening factor, $S_f(z) = \int_0^z F[c_{\text{Na}^+}(z) - c_{\text{Cl}^-}(z)] dz / |\sigma_s|$, where F is the Faraday constant. $S_f(z) > 1$ corresponds to an overscreening of the surface charge.

Figure 2 shows the variation of water and ion concentration as well as the screening factor across the channel. Apart from the well-known layering of water near the channel wall [9], we also observe that (1) a significant amount of Na^+ ions are accumulated within only 0.5 nm from the channel wall, (2) the concentration of Cl^- ion is very low in the region $z < 0.5$ nm even though its access to the region $0.35 \text{ nm} < z < 0.5$ nm is not limited by its

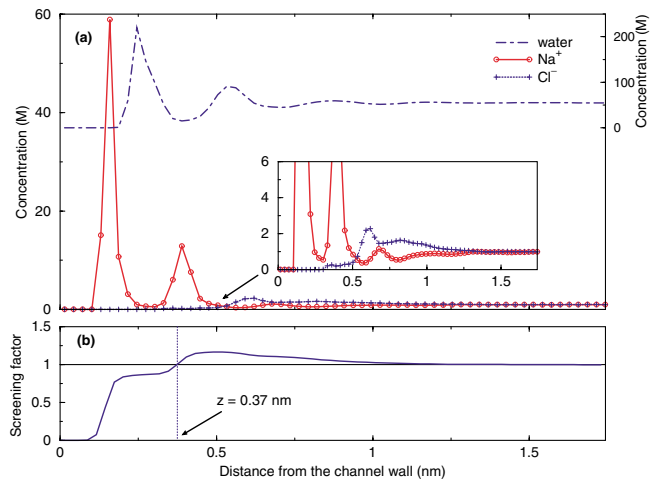


FIG. 2 (color online). Water/ion concentration profiles and the screening factor $S_f(z)$ across the channel (only the lower portion of the channel is shown because of the symmetry).

finite size [6], and (3) the surface charge is overscreened at a position of 0.37 nm away from the channel wall [i.e., $S_f(z) \geq 1$ for $z > 0.37$ nm] and charge inversion occurs in the region $z > 0.53$ nm. The overscreening and charge inversion cannot be predicted by the classical EDL theories, e.g., the Poisson-Boltzmann equation.

Observation (1) can be understood by analyzing the mean force acting on a Na^+ ion as shown in Fig. 3. From the PMF definition and the Boltzmann distribution, it follows that the accumulation of the Na^+ ions in the region $z < 0.5$ nm is mainly caused by the negative total mean force in regions II and IV of Fig. 3(a). Figure 3(a) also shows that the nonelectrostatic Na^+ -water interactions contribute significantly to the negative total mean force in these regions (the mean force due to the

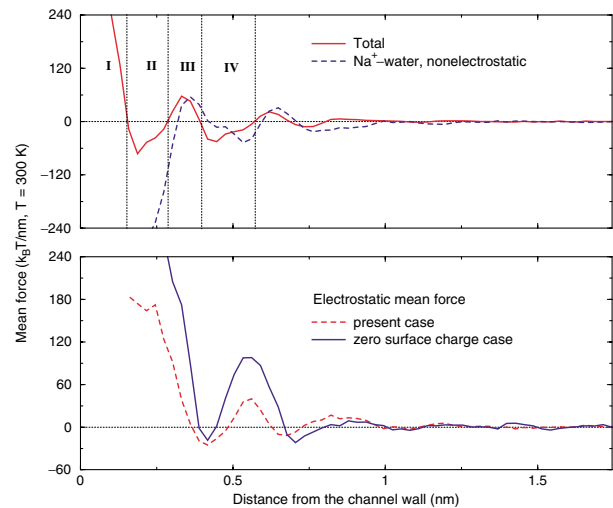


FIG. 3 (color online). (a) Total mean force acting on a Na^+ ion and its component due to the nonelectrostatic Na^+ -water interactions, (b) the electrostatic mean force acting on a Na^+ ion with and without the surface charge density. The zero surface charge case has the bulk ion concentration of 1.0 M.

nonelectrostatic interactions between $\text{Na}^+ - \text{Na}^+$, $\text{Na}^+ - \text{Cl}^-$, and $\text{Na}^+ - \text{wall}$ is not shown as their contribution to the total mean force is less significant). The magnitude and sign of the nonelectrostatic $\text{Na}^+ - \text{water}$ mean force depends mainly on the repulsive nonelectrostatic interactions between the Na^+ ion and its nearby water molecules and on the asymmetrical distribution of the water molecules around the ion (a symmetrical distribution will result in a zero mean force). For an ion located near the channel wall, the asymmetrical distribution of water molecules around the ion can be significantly influenced by the fluctuation of water concentration near the channel wall (see Fig. 2), which then leads to a fluctuating mean force in the region $0 < z < 0.75$ nm of Fig. 3(a).

The contribution of the electrostatic interactions is evaluated by studying the electrostatic mean force acting on the Na^+ ion, which is computed by subtracting the nonelectrostatic component from the total mean force. As shown in Fig. 3(b), the mean force acting on a Na^+ ion due to its electrostatic interaction with all other molecules in the system is positive for $z < 0.35$ nm. Such a positive mean force arises mainly from the fact that when the Na^+ ion is very close to the lower channel wall, the electrostatic interactions between the ion and its hydration water molecules, which are distributed mainly above the ion, tend to “pull” the ion from the surface. To understand how the surface charge contributes to the accumulation of Na^+ ions near the charged channel wall, we computed the electrostatic mean force experienced by a Na^+ ion in a reference case, where the surface charge density is zero and the bulk ion concentration is the same as in the present case. Figure 3(b) shows that when the surface is charged, though the electrostatic mean force acting on the Na^+ ion near the wall is positive, it is significantly lower compared to the case when the surface is not charged. From this we see that when the molecular nature of water is considered, the electrostatic interactions contribute to the accumulation of Na^+ ions near the charged channel wall in a different way from what one would expect in a classical EDL theory.

Observation (2), which deals mainly with the low Cl^- ion concentration in the region $z < 0.5$ nm, can be explained by performing an analogous mean force analysis for the Cl^- ion. Figure 4 shows that the total mean force acting on a Cl^- ion is strongly positive in the region $0.4 \text{ nm} < z < 0.6 \text{ nm}$ [see panel (a)], and it is dominated by the nonelectrostatic interactions between the $\text{Cl}^- - \text{Na}^+$ ions [see panel (b)] and $\text{Cl}^- - \text{water}$ molecules [see panel (c)]. This indicates that the low concentration of Cl^- ion in the region $0.35 \text{ nm} < z < 0.5 \text{ nm}$ is mainly caused by the nonelectrostatic interactions between $\text{Cl}^- - \text{Na}^+$ and $\text{Cl}^- - \text{water}$. The depletion of Cl^- ion in the region $z < 0.35$ nm is caused by the finite size of the Cl^- ion and has been explained in [6].

Observation (3), which deals with the overscreening and charge inversion, can be explained by the following two mechanisms. First, as discussed above, in addition to

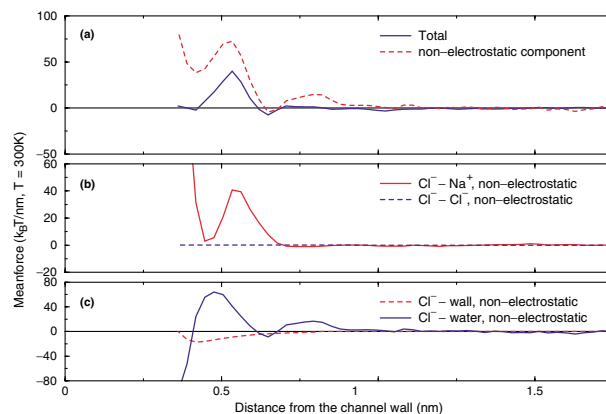


FIG. 4 (color online). (a) Total mean force acting on a Cl^- ion and its nonelectrostatic component, (b) and (c) are the mean forces experienced by a Cl^- ion due to its nonelectrostatic interactions with Na^+ and Cl^- ions, wall atoms, and water molecules.

the electrostatic interactions, the nonelectrostatic $\text{Na}^+ - \text{water}$ interactions also contribute significantly to the accumulation of Na^+ ions near the channel wall. Together, these interactions bring many more Na^+ ions towards the channel wall than what is predicted by the classical EDL theory, where the molecular nature of water is not considered. Second, because of the nonelectrostatic interactions between the Cl^- ions and the wall atoms and the water molecules, and because of the accumulation of Na^+ ions near the channel wall, the Cl^- ions tend to stay away from the channel wall and accumulate in the region $z > 0.5$ nm. The combination of these two mechanisms then makes it possible for the surface charge to be overscreened at a short distance from the channel wall ($z = 0.37$ nm), and for the concentration of Cl^- ion to exceed that of the Na^+ ion at a distance of 0.53 nm away from the channel wall. Though the second mechanism has been explored previously [8], the importance of the first mechanism is not widely understood. In fact, the influence of the molecular nature of water on the ion distribution in EDL is beginning to draw significant attention only recently [20,21].

Figure 5(a) shows the water velocity profile across the channel obtained by using molecular dynamics (MD) and continuum calculations [3]. In the continuum calculation, Poisson-Boltzmann (PB) equation is solved to obtain the ion concentration, which is then used to calculate the driving force for the flow given by the expression, $F_d(z) = e[c_{\text{Na}^+}(z) - c_{\text{Cl}^-}(z)]E_{\text{ext}}$, where e is the electron charge. $F_d(z)$ is used as the driving force in the Stokes equation [3] to compute the water velocity. In solving the PB equation, the bulk concentration of the NaCl solution is taken to be 1.0 M, which is consistent with the result shown in Fig. 2. For the Stokes equation, a nonslip boundary condition is applied at positions $z = 0.13$ and 3.36 nm, which is consistent with the MD observation. As discussed in [6], the dielectric constant and the viscosity of the water are taken as 81 and

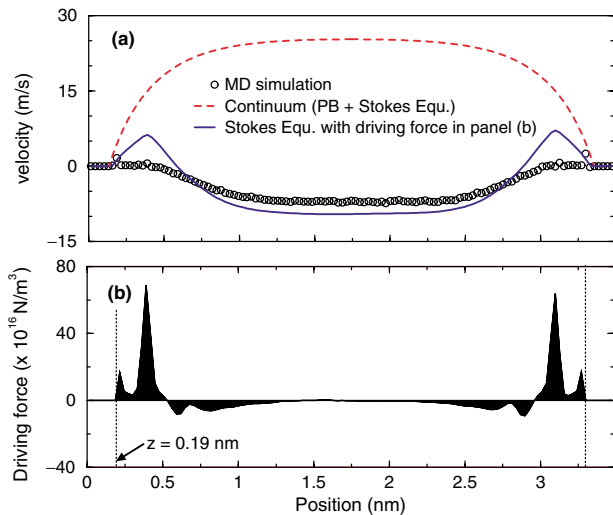


FIG. 5 (color online). (a) Water velocity profile across the channel obtained from MD and continuum simulations. (b) Driving force for the flow across the channel using the ion concentrations obtained from MD simulation.

0.743 mPa · s, respectively. From Fig. 5(a), we observe that while the continuum theory based on the PB and the Stokes equations predicts a positive velocity in the entire channel, the MD simulation shows a velocity that is slightly positive near the channel wall, but is negative in the region $0.42 \text{ nm} < z < 3.01 \text{ nm}$. Clearly, a flow reversal is observed, which cannot be explained by the “superequivalent specific adsorption” of counterions [9], as the Na^+ ions adsorbed on the channel wall did not overscreen the surface charge [see Fig. 2(b)]. To understand the flow reversal, we calculate the driving force, $F_d(z)$, for the flow using the ion concentration obtained from the MD simulation. Specifically, in the region where the ions are immobilized, $F_d(z)$ is taken as zero, and in the rest of the channel, $F_d(z)$ is computed by the expression given above, using the ion concentrations shown in Fig. 2. Figure 5(b) shows the calculated driving force. $F_d(z)$ is zero within 0.19 nm from the channel wall as the Na^+ ions adsorbed on the wall are immobilized (this was confirmed by analyzing the ion trajectory and may be due to the electrofriction between the counterions and the charged surface atoms as shown in [22]). Notice that because of the charge inversion, $F_d(z)$ is negative in the region $0.53 \text{ nm} < z < 2.96 \text{ nm}$. Figure 5(a) also shows the velocity computed by substituting the driving force obtained from the MD ion concentrations into the Stokes equation. Clearly, the new driving force can predict the flow reversal in the region $0.58 \text{ nm} < z < 2.91 \text{ nm}$, which indicates that the major mechanism for the flow reversal is the immobilization of the adsorbed Na^+ ion on the channel wall and the charge inversion. The velocity profile with the new driving force, however, still deviates from the MD velocity profile, especially in the regions close to the channel wall. The reason for this

deviation is not clearly understood at present, but is probably caused by the high local viscosity in the near wall region [6] although further investigation is needed before a definite conclusion can be drawn.

In summary, the charge inversion and flow reversal of electro-osmotic transport in a slit nanochannel was studied by using MD simulation. The molecular nature of water and ions, which was not accounted for in the continuum theories for EDL, is found to contribute significantly to the charge inversion. The flow reversal is mainly caused by the immobilization of Na^+ ions adsorbed on the channel wall and due to the charge inversion phenomena.

*Corresponding author.

Electronic address: <http://www.staff.uiuc.edu/~aluru>

- [1] D. J. Harrison *et al.*, *Science* **261**, 895 (1993).
- [2] T. C. Kuo *et al.*, *Anal. Chem.* **75**, 1861 (2003).
- [3] R. Probstein, *Physicochemical Hydrodynamics* (John Wiley & Sons, Inc., New York, 1994).
- [4] P. Kekicheff *et al.*, *J. Chem. Phys.* **99**, 6098 (1993).
- [5] J. B. Freund, *J. Chem. Phys.* **116**, 2194 (2002).
- [6] R. Qiao and N. R. Aluru, *J. Chem. Phys.* **118**, 4692 (2003).
- [7] R. Qiao and N. R. Aluru, *Nano Lett.* **3**, 1013 (2003).
- [8] H. Greberg and R. Kjellander, *J. Chem. Phys.* **108**, 2940 (1998).
- [9] J. Lyklema, *Fundamentals of Interface and Colloid Science* (Academic Press, San Diego, 1995).
- [10] J. Israelachvili, *Intermolecular and Surface Forces* (Academic Press, New York, 1992).
- [11] H. Poppe, A. Cifuentes, and W. Kok, *Anal. Chem.* **68**, 888 (1996).
- [12] D. E. Smith and L. X. Dang, *J. Chem. Phys.* **100**, 3757 (1994).
- [13] E. Lindahl, B. Hess, and D. van der Spoel, *J. Mol. Model.* **7**, 306 (2001).
- [14] S. Nose, *Mol. Phys.* **52**, 255 (1984).
- [15] J. L. Barrat and L. Bocquet, *Phys. Rev. Lett.* **82**, 4671 (1999).
- [16] I. Yeh and M. Berkowitz, *J. Chem. Phys.* **111**, 3155 (1999).
- [17] A strong external electric field can induce noticeable water alignment along the field direction, which can influence the ion distribution. To understand how this influences our result, we performed a simulation with zero external field. The ion distribution is found to be only slightly different from what is reported here and the charge inversion is still observed.
- [18] R. Kjellander and H. Greberg, *J. Electroanal. Chem.* **450**, 233 (1998).
- [19] D. Chandler, *Introduction to Modern Statistical Mechanics* (Oxford University Press, New York, 1987).
- [20] Y. Burak and D. Andelman, *Phys. Rev. E* **62**, 5296 (2000).
- [21] S. T. Cui and H. D. Cochran, *J. Chem. Phys.* **117**, 5850 (2002).
- [22] R. R. Netz, *Phys. Rev. Lett.* **91**, 138101 (2003).